Supporting Information for **Microsecond Charge Separation at Heterojunctions Between Transition Metal Dichalcogenide Monolayers and Single-Walled Carbon Nanotubes**

Dana B. Sulas-Kern, Hanyu Zhang, Zhaodong Li, Jeffrey L. Blackburn

National Renewable Energy Laboratory, Golden, Colorado 80401, United States

Materials and Methods

Wafer-Scale MoS_2 Monolayer CVD Growth. The MoS_2 growth procedures were adopted and modified from the previous methods developed by Yu and Liao et al.[1] The overall growth can be described as a low-pressure growth with the assistant of O_2. Chemical vapor deposition (CVD) was performed in a three-temperature-zone furnace with a dedicated insert tube to supply 25 sccm Ar/O_2 (4 vol. % of O_2) premixing gas flow directly to Zone 2. Zone 1 contained 500 mg of sulfur (Sigma Aldrich), and the sapphire wafer (UniversityWafer) was located at Zone 3. 2 mg of MoO_3 (Sigma Aldrich) was loaded into the insert tube and placed into Zone 2 of the furnace. 125 sccm of Ar was supplied to the growth chamber to carry the sulfur and balance the growth pressure at 1 Torr. The precursor MoO_3 in the insert tube with O_2 flow can prevent the poison of the MoO_3 precursor. During the growth, Zone 1, 2, 3 had the temperature ramping-up speeds of 35, 35, and 70 °C/min, and maintained temperatures as 180, 530, and 930 °C, respectively, for 30 min. After monolayer MoS_2 growth, the samples were broken into smaller ~1 cm^2 pieces for further characterization and spectroscopic studies.

(6,5) SWCNT / PFO-BPy Ink Preparation. Single-walled carbon nanotubes (SWCNTs, CoMoCAT SG65i, CHASM) were added in a concentration of 0.5 mg/mL to a solution of 2 mg/mL poly-[(9,9-dioctylfluorenyl-2,7-diyl)-*alt*-co(6,60-[2,20-bipyridine])] (PFO-BPy, American Dye Source) in toluene. The SWCNTs were dispersed using a Cole-Palmer CPX 750 tip sonicator with 0.5-inch diameter at 40% intensity for 15 minutes in a bath of flowing water. The dispersion was centrifuged for 5 minutes at 13,200 rpm and 20 °C in a Beckman Coulter L-100 XP ultracentrifuge with SW 32 Ti rotor to generate a compacted pellet and supernatant rich in (6,5) SWCNTs. The pellet was discarded, and the supernatant was centrifuged for an additional 16 hours at 24,100 rpm and 20 °C to generate a compacted pellet of (6,5) SWCNTs and supernatant containing excess PFO-BPy polymer. The supernatant was removed, and the (6,5) SWCNT pellet was gently rinsed with toluene before being redispersed in toluene using a heated ultrasonic bath sonicator. The polymer-removal centrifugation and subsequent redispersion were repeated twice.

(6,5) SWCNT Thin Film Deposition. MoS_2/SWCNT heterojunctions were prepared by spray coating the SWCNT ink onto MoS_2/sapphire substrates, and neat films were prepared by spray coating onto glass substrates that were cleaned by sequential sonication in acetone and isopropyl alcohol. The substrates were placed onto a motorized metal stage that was heated to 130 °C to evaporate solvent during the deposition. Prior to spray coating, the (6,5) SWCNT / PFO-BPy ink was diluted in toluene to reach an optical density of ~2.0 at the 1000 nm SWCNT S_{11} absorption peak. The ink was loaded into a syringe and injected at a rate of 0.3 mL/min through a SonoTek ultrasonic spray tip operated at 0.8 W. The ink mist was directed toward the substrates by N_2 at a flow rate of 7.0

standard liters per minute, and the substrates were rastered beneath the mist to achieve 20-30 coats. The resulting films were soaked in toluene at 78 °C for 10 minutes to remove excess polymer.

Transient Absorption Spectroscopy. Pump pulses were generated with a tunable-wavelength Light Conversion Topas optical parametric amplifier using input from a Coherent Libra Ti:Sapphire laser (800 nm, 100 fs, 1 kHz). White-light supercontinuum probe pulses for ultrafast measurements (hundreds of femtosecond to 5.5 ns delays) were generated by focusing a portion of the Ti:Sapphire output onto a sapphire plate. The pump-probe delay for the ultrafast time range was set using a mechanical translation stage prior to white light generation. Detection and data acquisition were carried out using the HELIOS system purchased from Ultrafast Systems Inc. For the nanosecond to microsecond time range, white-light probe pulse generation and electronic delays were carried out using the EOS system purchased from Ultrafast Systems Inc. Samples for transient absorption measurements were isolated from atmosphere by mounting them inside a double-window chamber that was sealed inside a nitrogen glovebox. The pump pulses used in this study were 1000 nm (0.6 μJ cm^{-2}) and 440 nm (4.6 μJ cm^{-2}), which generated approximately 1.1×10^{12} and 2.3×10^{12} absorbed photons cm^{-2}, respectively.

Steady-State Absorption. Ground-state absorption spectra were recorded using a Varian Cary 5000 spectrophotometer with baseline correction.

Raman and Photoluminescence. Measurements were carried out using an inVia Renishaw confocal Raman microscope with a 532 nm laser and a 50x objective lens. Raman scattering was detected using a grating with 1800 lines/mm, and photoluminescence was recorded using a grating with 600 lines/mm.

Atomic Force Microscopy. MoS_2 height profiles were obtained using a Bruker Innova atomic force microscope in contact mode measured across a scratch in the monolayer.

Additional Transient Absorption Global Analysis

Additional Fitting and Discussions

Figure S1 shows the normalized species-associated spectra from our global target analysis, using the heterojunction with 440 nm excitation as an example. Although global target analysis of the charge-associated decay requires three exponential components to fit the data, Figure S1 shows that all three charge-associated components have a similar spectral shape that is characteristic of charge on the SWCNT layer, including the trion induced absorption at 1175 nm and the S_{11} bleach at 1000 nm. The singlet-associated component has a different spectral shape with only the S_{11} bleach and no contribution from the 1175 nm induced absorption.

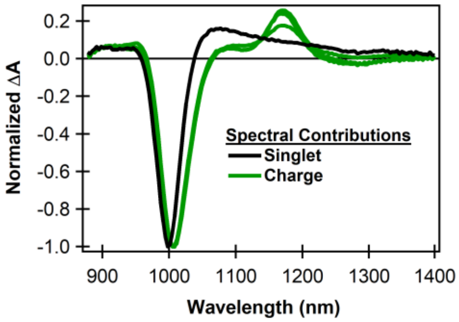

Figure S1. Normalized species-associated spectra showing similar spectral shape for all three charge-associated components.

Figure S2a-c show the kinetics at the SWCNT trion induced-absorption peak (1175 nm), where the data is given as light blue points and the total fit to the data is shown as a solid blue trace. The total fit is made up of the exciton-associated (black trace) and charge-associated (green trace) components, and the green dotted lines represent the three exponential components of the charge-associated decay. As shown in Figure S1, the three charge-associated components have similar spectral shape. Our fitting results for the heterojunctions in Figure S2 give faster rise time for charge carriers following 440 nm excitation (0.5 ps) and slower rise time with 1000 nm excitation (0.8 ps). The fit for the neat SWCNTs is dominated by the exciton-associated signal rather than charge carriers, although there is still a small amount of charge generation even in the neat SWCNTs. Figures S2d-f show the spectra at 1 ps overlaid with the fitting results. These results show that the heterojunction spectra are dominated by charge-associated signal even at early time delays, while the neat SWCNTs have a more significant contribution from singlet excitons.

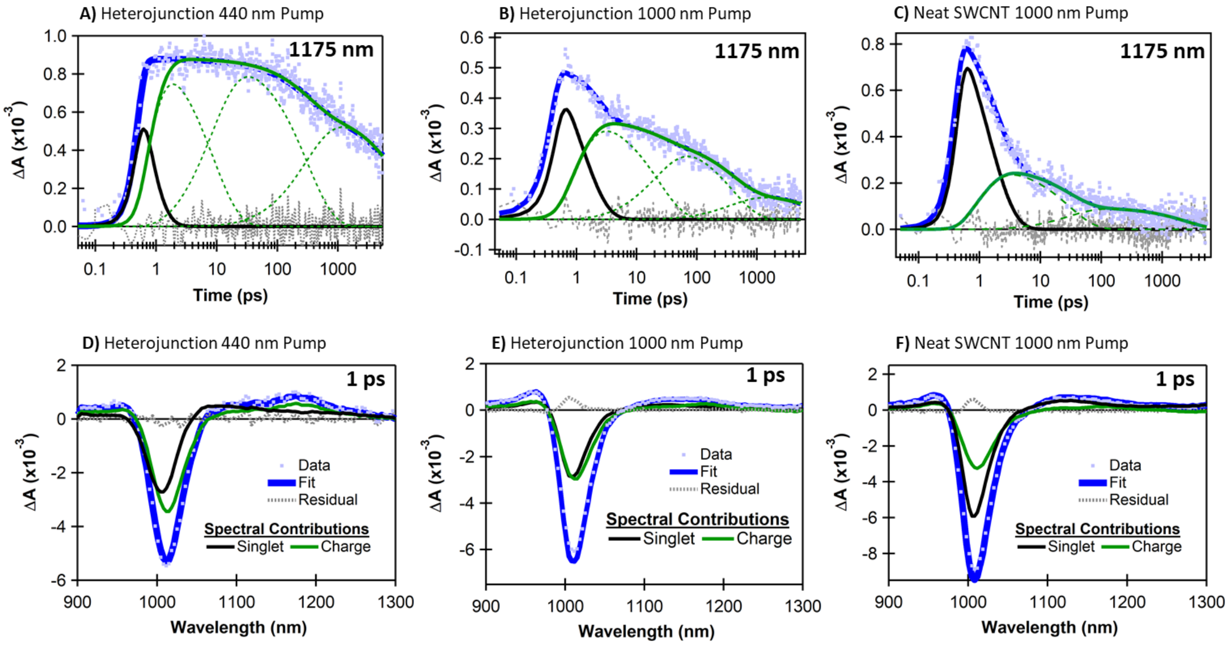

Figure S2. Kinetics data at 1175 nm (light blue points) overlaid with the time-dependent profiles corresponding to the singlet-associated (black trace) and charge-associated (green trace) spectral components which are summed to create the total fit (blue trace) giving minimal residual fitting error (gray dotted trace) for a) the MoS_2/SWCNT heterojunction with 440 nm excitation, b) the heterojunction with 1000 nm excitation, and c) the neat SWCNTs with 1000 nm excitation. Corresponding Transient absorption spectra at 1 ps (light blue points) are overlaid with the species-associated spectral components and total fit (blue trace) with associated minimal residual fitting error (gray dotted trace) for d) the MoS_2/SWCNT heterojunction with 440 nm excitation, e) the heterojunction with 1000 nm excitation, and f) the neat SWCNTs with 1000 nm excitation.

In Figure 6a of the main text, we show the MoS_2 species-associated spectral components in the heterojunction from a sequential kinetic model. We note that the rise time of 0.9 ps for the second MoS_2 species-associated component discussed in Figure 6a of the main text appears to be slower than the charge-transfer time (0.5 ps) obtained from our analysis of the SWCNT TA signals in Figure 4. We attribute the slower rise time for this MoS_2 charge-associated component to the possibility that our fitting procedure is unable to separate two simultaneous singlet decay processes with very similar time constants when species-associated components have the same spectral shape. That is, we suspect that singlets decay via both hole transfer (~0.5 ps, from the SWCNT charge-associated rise time) and carrier trapping (~1 ps),[2] which are represented in our analysis of the MoS_2-associated components by an average time constant. We also note that the charge-associated component with 0.9 ps rise time and 31 ps decay time exhibits a blue-shifted lineshape with a new induced absorption at 630 nm along with a slight decrease in the relative A exciton bleach magnitude compared to the B exciton bleach. We interpret this spectral shape of the charge-associated component to be consistent with a Stark effect. We note that the relatively long decay time that we observe is in contrast to the previous assignment of this spectral shape to hot states in MoS_2 that decay on sub-picosecond timescales.[3]

Charge-Transfer Yield

We estimate charge-transfer yields using an empirically-determined relationship for the trion absorption cross section.[4] Figure S3 shows our gaussian fits to the trion induced absorption of the SWCNT charge-associated spectral components from our global target analysis, where we use the area under the curve to obtain the relative trion optical density as $OD(X^+)/OD(S_{11})$. The fitting parameters are given in Table S1. The two traces for each graph in Figure S3 represent two charge-associated spectral components from the tri-exponential fit, which both contribute to the total fit of the charge-associated signal in different concentrations at the time of maximum trion amplitude. To calculate the total optical density of the trion-associated induced absorption, we multiply each component by its respective concentration at the time when the charge-associated signal is maximized, and we sum the contributions from the two components to get the total trion induced absorption amplitude.

We use the relative trion optical density $OD(X^+)/OD(S_{11})$ to find the hole concentration according to[4]

$$\frac{OD(X^+)}{OD(S_{11})} = 0.0674 - 0.0676 * Exp(-21.5\, N_h), \tag{S1}$$

where N_h is the hole density nm^{-1} of tube length. We convert the units to cm^{-2} of pump area using

$$N_h[cm^{-2}] = N_h[nm^{-1}]\frac{OD_{S11}}{\sigma\, N_c} \tag{S2}$$

where the absorption cross section σ is 1.5×10^{-17} cm^2 $atom^{-1}$ and the atomic density per nanometer of tube length N_C is 90.613 atoms nm^{-1}.[5] We then determine the CT yield as N_h/N_X, where N_X is the initial exciton concentration from the number of absorbed photons in the pump area.

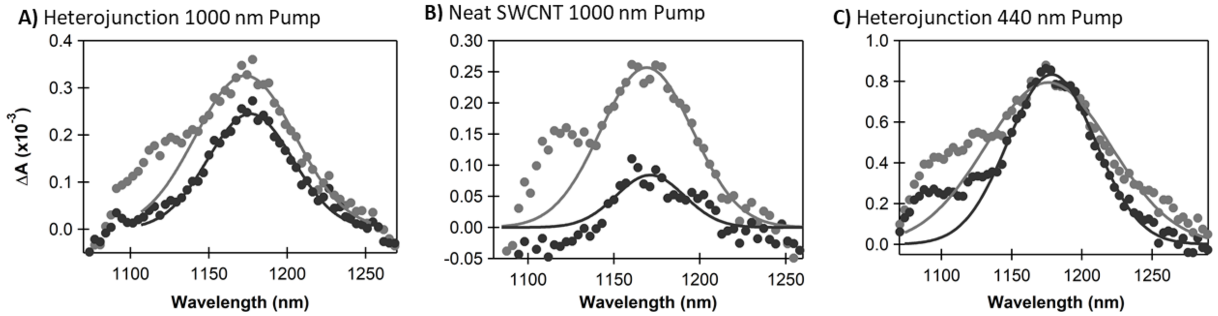

Figure S3. Gaussian fits of the trion induced absorption from the charge-associated spectral components obtained with global target analysis of our transient absorption data.

Table S1. Fitting parameters used to calculate the relative trion optical density for analysis of charge-transfer yields.

	Neat SWCNT 1000 nm Pump	**SWCNT MoS$_2$ 1000 nm Pump**	**SWCNT MoS$_2$ 440 nm Pump**
Trion1			
y_0	0	0	0
A	2.57E-04	3.26E-04	7.94E-04
x_0	1169	1173.3	1176
width	37.902	45.046	63.178
area	2.44E-02	3.68E-02	1.26E-01
adjusted for timetrace	2.20E-02	3.31E-02	1.07E-01
Trion2			
y_0	0	0	0
A	8.41E-05	2.45E-04	8.34E-04
x_0	1171.1	1176.4	1178.5
width	28.082	38.473	44.021
area	5.92E-03	2.36E-02	9.20E-02
adjusted for timetrace	4.14E-04	1.89E-03	1.01E-02
S_{11}			
y_0	0	0	0
A	1.01E-01	9.39E-02	9.39E-02
x_0	1002.1	1002.2	1002.2
width	31.58	32.559	32.559
area	8.02E+00	7.66E+00	7.66E+00
OD(X^+)/OD(S_{11})	**2.79E-03**	**4.57E-03**	**1.53E-02**

Fitting Coefficients for Long-Lived Carriers

We fit the charge carrier decay in Figure 3 of the main text using triple exponential, and we show the fitting parameters shown in Table S1. We use these parameters to calculate the amplitude-weighted average charge recombination lifetime as $\tau_{CR} = (A_1\tau_1 + A_2\tau_2 + A_3\tau_3) / (A_1 + A_2 + A_3) = 0.73$ μs.

Table S1. Triple exponential fitting parameters

A	**τ (μs)**	**Amplitude Percent**
0.34820	0.01754	43.2353
0.34240	0.23300	42.5151
0.11476	4.38020	14.2495

References

1. Yu, H.; Liao, M.; Zhao, W.; Liu, G.; Zhou, X. J.; Wei, Z.; Xu, X.; Liu, K.; Hu, Z.; Deng, K.; Zhou, S.; Shi, J.-A.; Gu, L.; Shen, C.; Zhang, T.; Du, L.; Xie, L.; Zhu, J.; Chen, W.; Yang, R.; Shi, D.; Zhang, G., Wafer-Scale Growth and Transfer of Highly-Oriented Monolayer MoS2 Continuous Films. *ACS Nano* **2017,** *11* (12), 12001-12007.
2. Bettis Homan, S.; Sangwan, V. K.; Balla, I.; Bergeron, H.; Weiss, E. A.; Hersam, M. C., Ultrafast Exciton Dissociation and Long-Lived Charge Separation in a Photovoltaic Pentacene–MoS2 van der Waals Heterojunction. *Nano Lett.* **2017,** *17* (1), 164-169.
3. Zhong, C.; Sangwan, V. K.; Wang, C.; Bergeron, H.; Hersam, M. C.; Weiss, E. A., Mechanisms of Ultrafast Charge Separation in a PTB7/Monolayer MoS2 van der Waals Heterojunction. *J. Phys. Chem. Lett.* **2018,** *9* (10), 2484-2491.
4. Dowgiallo, A.-M.; Mistry, K. S.; Johnson, J. C.; Blackburn, J. L., Ultrafast Spectroscopic Signature of Charge Transfer between Single-Walled Carbon Nanotubes and C60. *ACS Nano* **2014,** *8* (8), 8573-8581.
5. Blackburn, J. L.; Ferguson, A. J.; Reid, O. G., Spectroscopy of Ground- and Excited-State Charge Carriers in Single-Wall Carbon Nanotubes. In *Handbook of Carbon Nanomaterials*, World Scientific: 2017; Vol. Volume 9 & 10, pp 237-296.